# Translational pharmacokinetics-pharmacodynamics in zebrafish: integration of experimental and computational methods

Wijk, R.C. van

Chapter 10

# Translational pharmacokinetics-pharmacodynamics of isoniazid in the zebrafish larva tuberculosis disease model

Rob C. van Wijk, Wanbin Hu, Sharka M. Dijkema, Dirk-Jan van den Berg, Jeremy Liu, Rida Bahi, Fons J. Verbeek, Ulrika S.H. Simonsson, Herman P. Spaink, Piet H. van der Graaf, Elke H.J. Krekels

*Submitted*

## 10.1 One Sentence Summary

Internal drug exposure and antibacterial response in zebrafish larva as tuberculosis disease model are translated to predict the isoniazid exposure-response relationship in humans using pharmacokinetic-pharmacodynamic modelling.

## 10.2 Abstract

There is a strong need for innovation in anti-tuberculosis drug development. The zebrafish larva is an attractive disease model in tuberculosis research. However to translate pharmacological findings to higher vertebrates including humans, the internal exposure of drugs commonly dissolved in the external water, needs to be quantified and linked to observed response. We developed experimental methods to quantify internal exposure, including nano-scale blood sampling and to quantify the bacterial burden, using automated fluorescence imaging analysis, with isoniazid as paradigm compound. Internal exposure was only 20% of the external drug concentration. The bacterial burden grew exponentially and an external concentration of 75 mg/L (5x minimum inhibitory concentration) lead to bacteriostasis. We used pharmacokinetic-pharmacodynamic modelling to quantify the exposure-response relationship responsible for the antibiotic response. Based on this quantitative relationship, isoniazid response was translated to humans, which correlated well with observed data. This proof-of-concept confirms the potential of the zebrafish larvae as tuberculosis disease model in translational pharmacology.

## 10.3 Introduction

Tuberculosis (TB) is the leading cause of death from infectious diseases in adults and *Mycobacterium tuberculosis* is becoming the deadliest pathogens on the planet[1]. The United Nations Sustainable Development Goals aim to eradicate the TB epidemic before 2030[2], but progress is stalling due to ineffectiveness of currently available treatments[3]. Drug development is a challenging, lengthy, and costly process, generally requiring a decade for drugs to reach the market with estimated costs of 1-2.5 billion dollar per approved new drug[4]. Development of anti-TB drugs is especially difficult, with laboratory biosafety issues[5], slow replication rate of *M. tuberculosis*, and long duration of treatment and patient follow-up[6]. As a result, there is a strong need for innovations in the development of new TB treatments[6–8].

Phenotypic- and systems-based drug development both integrate experimental and computational innovation and utilizes whole organisms studies, preferably vertebrates, for quantitative translational purposes to open a new realm of possible discoveries overseen when focusing on single cell-type targets. High-throughput experiments within whole vertebrates may improve efficiency and effectiveness of drug development, and is possible with the zebrafish larva as model organism[9].

The zebrafish (*Danio rerio*) is increasingly used in biomedical research, because of its many advantages which include high fecundity, fast development, transparency throughout the first period of life, easy genetic modification, and limited ethical constraints[9–11]. Zebrafish larvae infected by *M. marinum*, a close

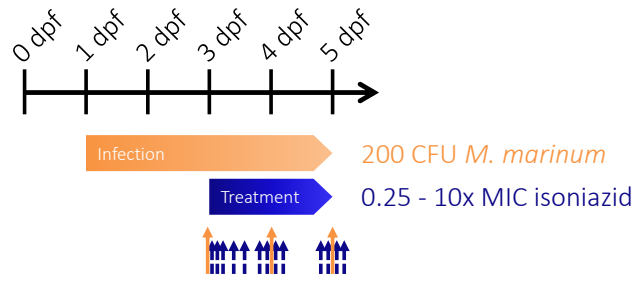


Figure 10.1 Experimental study design. Fertilized eggs at 0 days post fertilization (dpf) were harvested and injected with 200 CFU *M. marinum* at 1 dpf. After two days of establishing the infection, fluorescence imaging was performed (orange arrow, n ≥ 20 larvae per group) and the treatment with isoniazid dissolved in the external treatment medium (0.25-10x MIC, MIC = 15 mg/L, and control) was started. Fluorescence imaging was repeated daily (orange solid arrows). In separate animals groups, destructive homogenate (at least 3 replicates consisting of 5 larvae per dose per time point) and blood samples for internal isoniazid exposure quantification were taken from 0 to 50 hours of treatment (blue dashed arrows).

relative of *M. tuberculosis*, are an established TB disease model to study host-pathogen interaction[12–15] and to screen for novel drugs[16,17], with faster replication times and less biosafety risks than experiments with *M. tuberculosis*[18]. Imaging of zebrafish larvae infected with fluorescent mycobacteria[19,20] allows for repeated longitudinal measurements from individual larvae, which reduces overall noise in data as biological and experimental variability can be quantified separately. This is in contrast to *ex vivo* bacterial burden organ count by colony forming units (CFU) or MGIT liquid media systems currently utilized in preclinical TB research[21–23].

Translation of drug response between species is challenging and considerably limits drug development[24]. Currently, treatment of zebrafish larvae is performed by dissolving drugs into the water in which the larvae swim, without taking into account how much drug is actually taken up by the larvae. Translating pharmacological response between species however requires quantification of the drug exposure at the site of action as a basis for the quantification of the exposure-response relationship[25]. Although challenging because of their small size, we have developed new experimental methods to quantify internal drug exposure based on ultra-sensitive analytical techniques and a novel method for nanoscale blood sampling. Pharmacological model-based approaches can then be used to quantitatively link the internal exposure over time (pharmacokinetics) of anti-TB drugs to bactericidal response in the zebrafish larvae observed by fluorescence microscopy (pharmacodynamics). The exposure-response relationship that is thus obtained is the basis for translational pharmacology to higher vertebrates, including humans.

Here, for the first time, we present an integration of experimental and computational approaches in zebrafish larvae infected with *M. marinum* and treated with increasing waterborne isoniazid doses from 0.25-10x the minimum inhibitor concentration (MIC) (3.75-150 mg/L). The internal exposure is quantified in homogenates and blood samples of the larvae, and the bacterial burden is quantified by automated fluorescence image analysis (Figure 10.1). Pharmacokinetic-pharmacodynamic modelling is performed to quantify the exposure over time and the exposure-response relationship. Isoniazid is chosen because it is known to have the largest early bactericidal activity for single drug treatments among the current standard of care drugs against TB[26]. The quantified exposure-response relationship in the zebrafish larvae together with simulated concentration-time profiles in TB patients is utilized to translate the findings on isoniazid response in the zebrafish larvae to humans. A quantitative comparison with reported observations from patients is made as a proof of concept, to assess translational value of this new disease model in anti-TB drug development.

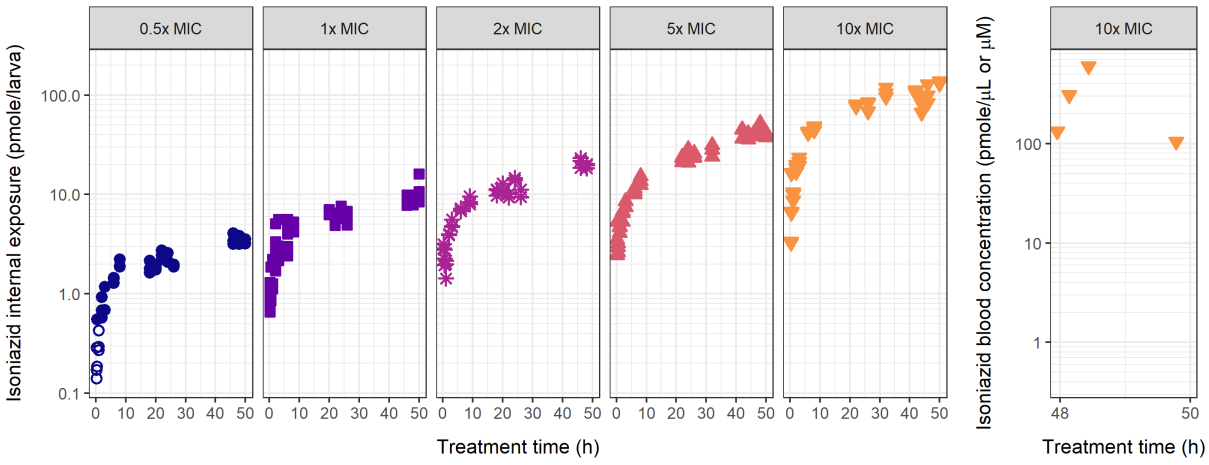


Figure 10.2 Internal isoniazid exposure over time in zebrafish larvae for increasing isoniazid doses. Internal exposure as pmole per larva in homogenate samples (left 5 panels) or as pmole/µL in blood samples (right panel) is shown on a semi-logarithmic scale for waterborne doses in the external treatment medium of 0.5 (blue circles), 1 (purple squares), 2 (lilac stars), 5 (orange upward triangles), and 10 (yellow downward triangles) x MIC (MIC = 15 mg/L) for a constant treatment period of 50 hours. Internal exposure linearly increases with dose, and steady state amounts increase with age, suggesting increased net absorption. Open symbols show observations below lower limit of quantification.

## 10.4 Results

*10.4.1 Internal exposure of isoniazid in zebrafish larvae*

Internal exposure of isoniazid in zebrafish larvae after constant treatment between day 3-5 post fertilization (dpf) with increasing doses of 0.5, 1, 2, 5, and 10x MIC (7.5, 15, 30, 75, and 150 mg/L) was quantified. Figure 10.2 showed a clear dose-linearity, where a 10-fold higher dose resulted in a 10-fold higher internal exposure. Internal exposure measured in homogenates reached steady state values within 12 hours and after that increases with age. To quantify the blood concentration in the zebrafish larvae of 5 dpf, an innovative novel blood sampling method was used. Median blood concentration of isoniazid at 48 hour of treatment (5 dpf) with 150 mg/L was 30.3 mg/L (221 µM, range 14.4-82.6 mg/L, Figure 10.2), meaning that the internal exposure to isoniazid was only 20% of the external concentration.

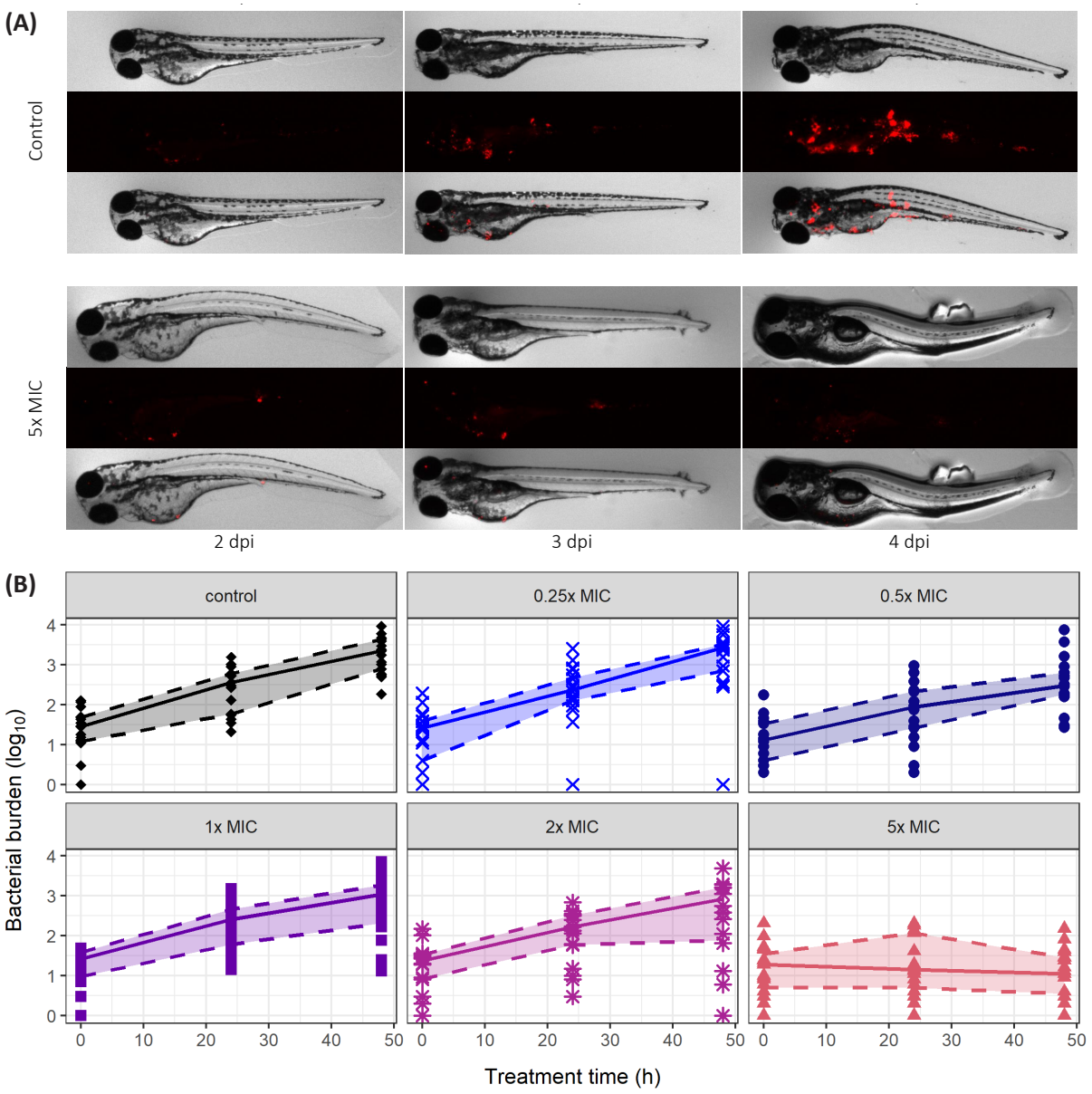


Figure 10.3 Bacterial burden quantified by fluorescence imaging. (A) Representative images (brightfield (top), red fluorescence channel (middle), overlay (bottom)) for control and 5x MIC treatment groups at 2, 3, and 4 dpi (MIC = 15 mg/L). (B) The bacterial burden in fluorescent pixel count quantified by automated image analysis for control and treatment groups with doses 0.25x – 5x MIC selected after feasibility study and taking into account fluorescence detection limit. Symbols represent observations, while lines represent median and quantiles, with the inter-quantile range as shaded area.

*10.4.2* M. marinum *bacterial burden in zebrafish larvae upon isoniazid treatment*

The bacterial burden of *M. marinum* was quantified through fluorescence imaging with repeated measurements per individual larva. Doses ranging from 0.25x to 5x MIC were chosen based on a feasibility study, and on the fluorescence detection limit. Figure 10.3 showed representative images of which the fluorescent pixels are quantified by automated image analysis software[19,27], based on pixel counts. The median and inter-quartile range of the bacterial burden clearly showed that bacterial growth is decreasing with increasing doses in comparison to the control. The highest dose of 5x MIC, which corresponded to 1x MIC internal exposure, showed a decline in the bacterial burden over time.

*10.4.3 Quantification of the exposure-response relationship for isoniazid in zebrafish larvae*

To quantify the exposure-response relationship, a sequential modelling approach was performed. First, the internal exposure over time was quantified in the pharmacokinetic component of the model, after which this was linked to the isoniazid response in the final pharmacokinetic-pharmacodynamic model (Figure 10.4).

A one-compartment model with first order absorption and first order elimination best described the data on internal exposure. Because the larvae are still developing, both absorption and elimination were expected to increase with age[28]. The data showed an increase in the steady state amounts with increasing age, suggesting that absorption rates increase faster than elimination rates. Because the impact of age on absorption and elimination were indistinguishable at steady state, we estimated a net effect as increase on absorption only. Age was included as predictor (covariate) on the absorption rate constant ($k_a$) in two ways: first, as exponential relationship per hour post fertilization (hpf), and second, based on knowledge on the physiology of the gastro-intestinal (GI) tract which opens between 3 and 4 dpf[29], as discrete increase at 4 dpf (Equation 1).

$$k_a = \begin{cases} k_{a,0} \cdot k_{a,hpf}^{\frac{age}{median(age)}} & age = 3\ dpf \\ k_{a,0} \cdot k_{a,hpf}^{\frac{age}{median(age)}} \cdot \left(1 + k_{a,GI}\right) & age \geq 4\ dpf \end{cases} \quad (1)$$

in which $k_{a,0}$ was the absorption rate constant at the median age of 101 hpf, $k_a$,hpf was the constant in the exponential covariate relationship, and $k_{a,GI}$ was the discrete factor with which the absorption rate constant increased at 4 dpf. A linear covariate relationship was statistically significantly worse ($p < 0.001$) compared to an exponential relationship, a power relationship was statistically similar ($p > 0.1$), but resulted in worse precision of the parameter estimates.

Precision of all pharmacokinetic parameters in the final model was acceptable (relative standard errors < 36%), with the exception of $k_{a,GI}$ (relative standard error of 51%). Removing the effect of the opening of

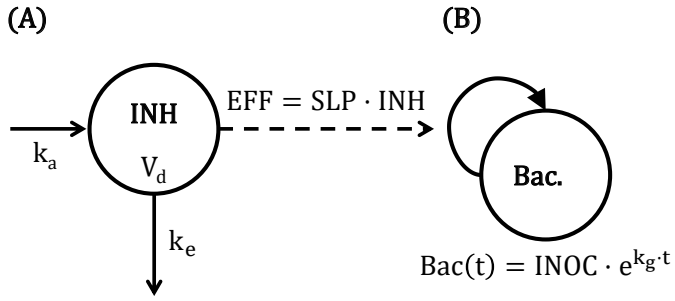


Figure 10.4 Schematic representation of the pharmacokinetic-pharmacodynamic model quantifying the internal exposure of isoniazid and its response on the bacterial burden in zebrafish larvae. Compartments represent drug concentration or number of bacteria inside the larva, solid straight arrows represent mass transfer, curved arrow represent bacterial growth, dashed arrow represents drug response. (A) shows the pharmacokinetic component of the model for isoniazid (INH) with a first order absorption rate constant ($k_a$) from the external treatment medium on which larval age is included as a covariate (Equation 1), distribution volume ($V_d$), and first order elimination rate constant ($k_e$). (B) shows the bacterial burden (Bac.) with exponential growth rate ($k_g$) as growth function and inoculum (INOC) at time point zero. Exposure-response relationship (EFF) is quantified with a linear model (SLP = slope).

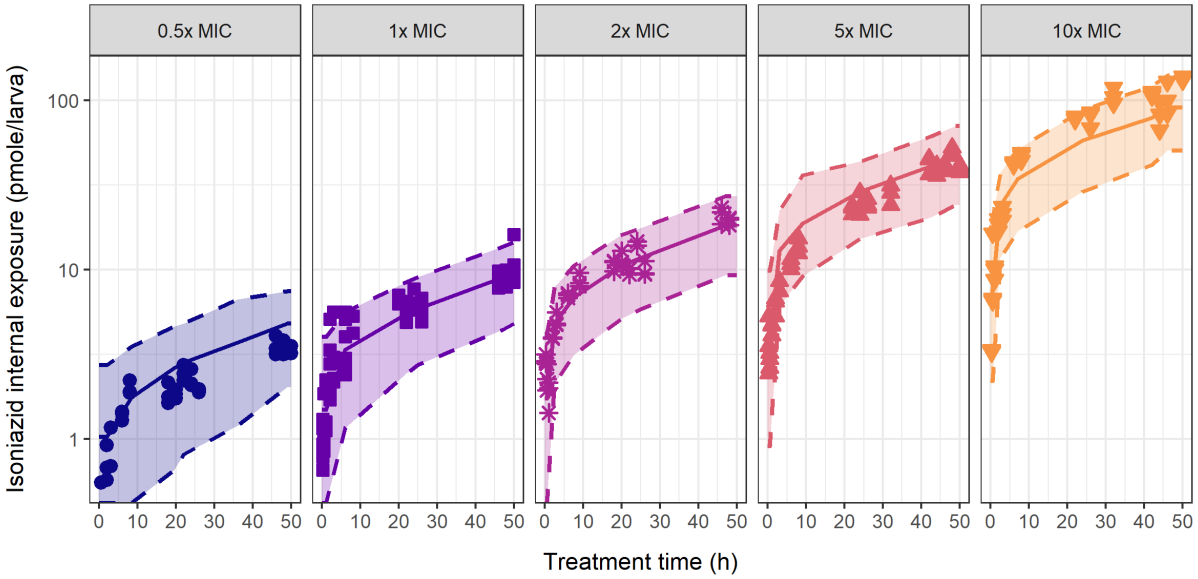


Figure 10.5 Model-based prediction of the internal isoniazid exposure in zebrafish larvae of the final pharmacokinetic-pharmacodynamic model. Median (solid line) and 95% prediction interval (dashed lines, shaded area) from 500 simulations based on the pharmacokinetic component of the final model show good prediction of the observed data (symbols) of internal exposure obtained after constant waterborne isoniazid treatment of 0.5 (blue circles and lines), 1 (purple squares and lines), 2 (lilac stars and lines), 5 (orange upward triangles and lines), and 10 (yellow downward triangles and lines) x MIC (MIC = 15 mg/L).

the GI-tract worsened the fit significantly ($p < 0.05$) and as the opening of the GI-tract was physiologically expected to impact absorption the relationship was retained despite the relative imprecision of the obtained estimate. The precision of the remaining model parameters confirmed that the obtained model and parameter values were supported by the data. Goodness-of-fit plots further confirmed an unbiased fit of the data by the model (Supplementary Figure S10.1). A visual predictive check was provided in Figure 10.5, which showed good prediction of the typical trends and a slight over-prediction of the variability of the observed data by the model.

The bacterial burden data was best described by an exponential growth model (Equation 2). The data did not support separate estimation of growth and decay, thus net growth was estimated. In case of bacterial kill, this net growth will be negative. A linear exposure-response relationship fitted the data best (Equation 6). The biological variability between larvae was quantified by inclusion of inter-individual variability on the inoculum (coefficient of variation 204%) and slope of the drug response (coefficient of variation 50.5%). The experimental variability was very reasonable with a coefficient of variation of 36.3%. The predicted isoniazid response in zebrafish larvae was shown in Figure 10.6 (individual predictions Supplementary Figure S10.2), with a clear increase in antibacterial response by the different doses which was in line with the observations. Goodness-of-fit plots showed unbiased model fit (Supplementary Figure S10.3). Parameter estimates of the final pharmacokinetic-pharmacodynamic model were given in Table 10.1.

### *10.4.4 Translation of isoniazid response to humans*

An exposure-response relationship of a drug can be assumed to be conserved between vertebrates[24,30–32]. As a proof of concept, the response of isoniazid in zebrafish larvae was translated to humans, assuming the isoniazid response on *M. tuberculosis* in humans to be similar to the isoniazid response on its close relative *M. marinum*. Translational factors regarding the difference in sensitivity to isoniazid as reported by MIC, and difference in stage of infection, were taken into account[31]. The exposure-response relationship quantified in the current study was linked to simulated isoniazid concentration-time profiles of patients from a previously published pharmacokinetic model for isoniazid[33]. Simulations with three human doses were performed; a sub- and a super therapeutic dose of 150 and 450 mg, in addition to the

Table 10.1 Parameter estimates including relative standard errors (RSE) of the final pharmacokinetic-pharmacodynamic model (Figure 10.4)

| | **Parameter value** | **RSE (%)** |
|---|---|---|
| *Pharmacokinetic structural parameters* | | |
| $k_{a,0}$ (µL/h$^{-1}$) | 0.00349 | 25 |
| $k_{a,hpf}$ (-) | 7.61 | 17 |
| $k_{a,GI}$ (-) | 0.171 | 51 |
| $k_e$ (h$^{-1}$) | 0.580 | 32 |
| $V_d$ (µL) | 0.325 | 36 |
| *Pharmacodynamic structural parameters* | | |
| $k_g$ | 0.0930 | 4 |
| Inoculum (Fluorescence) | 16.3 | 13 |
| Slope (µM$^{-1}$) | 0.00991 | 37 |
| *Pharmacodynamic inter-individual variability* | | |
| Variance of inter-individual variability Inoculum (-) | 1.64 | 18 |
| Variance of inter-individual variability Slope (-) | 0.227 | 93 |
| *Pharmacokinetic residual variability* | | |
| Variance of proportional error homogenate (-) | 0.0609 | 24 |
| Variance of additive error homogenate (pmole/larva) | 0.591 | 45 |
| Variance of proportional error blood (-) | 0.482 | 49 |
| *Pharmacodynamic residual variability* | | |
| Variance of proportional error (-) | 0.124 | 17 |

recommended dose of 300 mg. Reported observations of *M. tuberculosis* bacterial burden quantified in sputum after isoniazid monotherapy of daily 300 mg[34–36] served as quantitative comparison. Figure 10.7 shows the simulated concentration-time profile and the bacterial burden-time profiles for 1,000 virtual patients per dose group, the latter of which for a dose of 300 mg was in good agreement with the observed data. The simulations after sub-therapeutic dose of 150 mg showed limited isoniazid response and hence bacterial growth. The therapeutic dose of 300 mg showed a decline in the bacterial burden. The median translated bacterial burden declined 5-6 $\log_{10}$ CFU/mL during the 7 days treatment period, or 0.7-0.9 $\log_{10}$ CFU/mL/day. The super therapeutic dose of 450 showed a steeper decline of the bacterial burden.

The translated isoniazid response at the therapeutic dose correlated well with the observed data for the first 48 hours which was also the duration of treatment studied in the zebrafish larvae in this work. Extrapolating to later time points showed a slight over-prediction of isoniazid response, while the observations were still within the prediction interval. This proof-of-concept suggests that the zebrafish larva is a promising addition to the quantitative model-based translational pipeline in anti-TB drug development.

## 10.5 Discussion

There is a strong need for innovation in anti-TB drug development. With its high-throughput potential, its possibility for repeated fluorescence imaging to quantify infection, and its fast, cheap, and relatively safe experimentation, the zebrafish larva tuberculosis disease model combines the advantages of *in vitro* experiments within a whole-organism vertebrate. In this work, we developed an experimental approach to acquire data on the internal exposure, on the bacterial burden, and utilized computational pharmacokinetic-pharmacodynamic modelling to quantify the exposure-response relationship, which

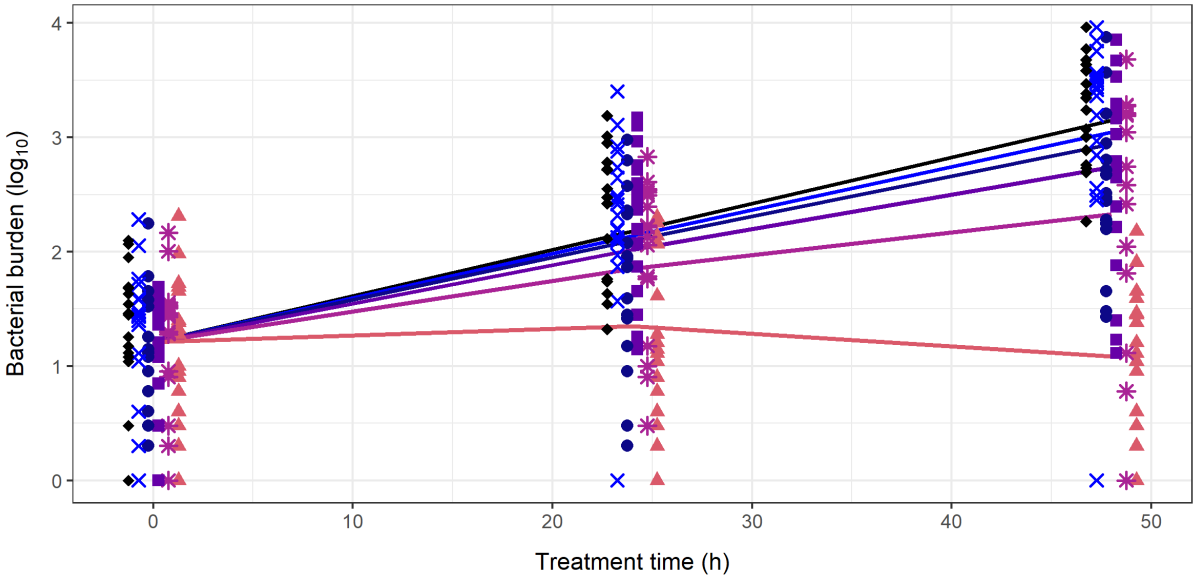


Figure 10.6 Model-based prediction of the bacterial burden after isoniazid treatment in zebrafish larvae infected with *M. marinum*. The bacterial burden as $log_{10}$-transformed fluorescent pixel count is shown over treatment time of 50 hours at isoniazid doses in the external treatment medium of 0.25 (light blue crosses and line), 0.5 (blue circles and line), 1 (purple squares and line), 2 (lilac stars and line), and 5 (orange upward triangles and line) x MIC (MIC = 15 mg/L), in addition to control (black diamonds and line). Symbols represent observed data, lines represent model prediction. Biological variability as quantified by the model is relatively large in contrast to experimental variability (see for individual predictions Supplementary Figure S10.2).

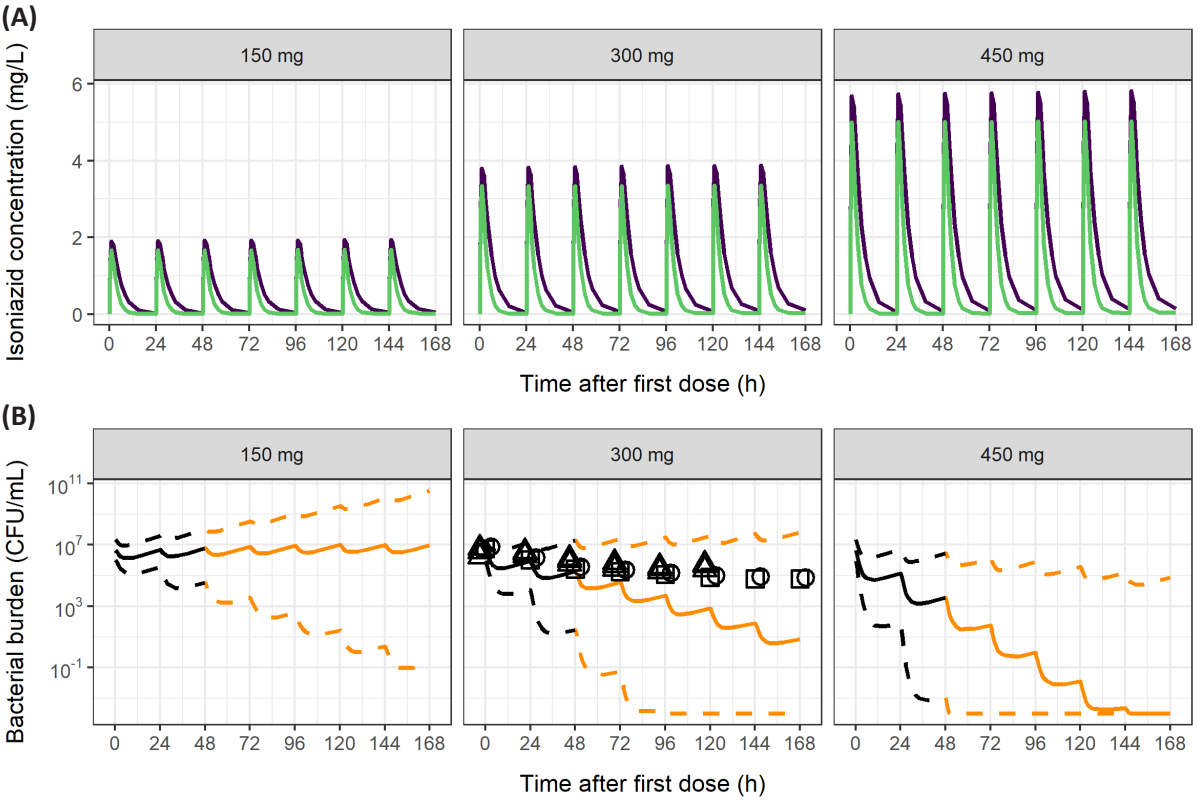


Figure 10.7 Translation of isoniazid response to humans based on final zebrafish pharmacokinetic-pharmacodynamic approach. (A) isoniazid concentration-time profile for a fast (green) and slow (purple) metabolizer typical individual after 7 days of daily isoniazid doses of 150 mg, 300 mg, and 450 mg as simulated from a previously published pharmacokinetic model[33]. (B) Simulated median (solid line) and 10th and 90th percentile (dashed lines) bacterial burden in CFU/mL sputum based on the human isoniazid concentration-time profile for 1,000 individuals per dose group and the exposure-response relationship quantified in zebrafish larvae, and translational factors on isoniazid sensitivity (MIC) and stage of infection (logarithmic vs stationary). Translated response corresponds well to the observed bacterial burden in sputum (circles[34], squares[35], triangles[36]). Orange part of the prediction is extrapolated in time from the 48 hours of treatment studied in the zebrafish, shown in black.

successfully translated to isoniazid response in humans. This translation to human response shows the strengths of quantifying internal exposure-response relationships, crucial for successful translational pharmacology in drug development. Using our workflow, zebrafish studies can bridge the gap between *in vitro* experiments and *in vivo* preclinical drug development, thereby increasing speed and improving quantitative understanding of *in vivo* drug response early in the drug development process. Through this quantitative model based approach, the zebrafish larva becomes a full member of the translational pipeline in drug development.

Quantification of internal exposure in zebrafish larvae after drug treatment is essential for reliable interpretation of drug response, but because of small sample volumes and low amounts this is not straight forward. We have built upon recent work to develop an ultra-sensitive liquid chromatography-mass spectrometry (LC-MS/MS) based quantification method, including derivatization[28,37,38]. This methodology proved sensitive enough to quantify isoniazid in larval homogenates and blood samples of only nanoliters in volume. The latter is especially of importance because blood concentrations are required to scale amounts in homogenates to concentrations, essential for inter-species translation. The state of the art blood sampling method is not yet high-throughput, but automation based on previously developed automated injection systems are under development[39].

Utilizing fluorescence imaging to establish the response of isoniazid on mycobacteria has clear advantages over CFU plating, as the latter has been reported to show large sample-to-sample variability[40]. An important advantage of fluorescence imaging in zebrafish larvae is the possibility of repeated longitudinal measurements of the bacterial burden within a single individual, which is uncommon in preclinical TB research. These repeated measurements not only suppress noise by distinguishing biological from experimental variability, but also reduce the number of subjects needed in an experiment, which is ethically preferable. Additionally, fluorescence imaging of bacteria does not require these bacteria to grow on solid- or in liquid media, and will include both multiplying and non-multiplying, i.e. dormant bacteria. Currently, the medium-throughput imaging set-up used here is restricted by its fluorescence detection limit to clearly quantify mycobacterial kill, which is why the highest dose of 10x MIC was not tested in the bacterial burden study. Imaging systems are continuously being improved, pushing the detection limit to the individual mycobacterium[41].

*M. marinum* and *M. tuberculosis* are sensitive to isoniazid to a different extent, as MIC against *M. marinum* ranges between 1.6 and 32 mg/L[42–45], in concordance the value obtained in our analysis, which is higher than the MIC against *M. tuberculosis* which ranges from 0.016 to 0.2 mg/L[23,46–49]. This difference in sensitivity was taken into account when predicting human efficacy by scaling the effective concentration with the ratio of MICs as scaling term which has earlier been shown as a method for handling strain differences[31]. The difference in stage of infection between the logarithmic growth of a fresh infection in the zebrafish here, and the stationary infection of patients starting treatment, was taken into account as well which has been shown to be an important translational factor[31].

The pharmacokinetic-pharmacodynamic model developed here was limited by the available data and is currently empirical in nature. The estimation of net absorption and net growth cannot be distinguished from the impact of age on absorption and elimination separately, or on the drug response on growth or kill, respectively. Parameterization as net absorption or growth can impact the interpretation of these parameters, so care must be taken. However, translation based on this empirical model was reasonable, and will further improve with the addition of more physiological or mechanistic details. A multistate tuberculosis pharmacometric (MTP) model has been developed previously for *M. tuberculosis*, quantifying *in vitro* natural growth over 200 days using a fast-, slow-, and non-multiplying subpopulation. The drug responses of isoniazid, rifampicin, and ethambutol have been quantified on these states[50,51] and successfully translated to mice[52,53] and patients[54]. This multistate approach, especially when the *in vitro* natural growth and time-kill is repeated for *M. marinum* as well, can be integrated with our analysis of *M. marinum* to strengthen the translational value of findings in zebrafish to higher vertebrates[55].

The reported bacterial burden in humans after 300 mg isoniazid monotherapy daily fell within the prediction interval obtained from simulated concentration-time profiles in humans and the exposure-response relationship quantified in zebrafish larvae here. The simulated decline in the bacterial burden of 0.7-0.9 $\log_{10}$ CFU/mL/day has been reported in humans before after 2 days of treatment[56]. The large variability in the prediction interval from this work was largely due to the high biological variability in the inoculum, resulting from the establishment of infection during the first two days, and the slope of the linear drug response quantified in zebrafish larva. Care must also be taken when extrapolating a linear exposure-response relationship to exposures outside the studied range, as well as extrapolating the response of treatment after the 48 hours of treatment in zebrafish larvae. The treatment duration was deliberately not extended beyond 48 hours, to remain within the ethically preferable age limit (Figure 10.1)[57].

In conclusion, we have developed a new experimental and computational approach to translate the pharmacokinetic-pharmacodynamic relationship of isoniazid in a zebrafish model of TB to human. We propose that this approach can be used in the search for novel TB regimens.

## 10.6 Materials and Methods

*10.6.1 Study design*

Zebrafish embryos of the VUmc wild type strain were dechorionated and infected with *M. marinum* strain E11 at 28 hpf and kept at 28°C throughout the experiment. At 2 days post infection (dpi), the bacterial burden in zebrafish larvae was quantified by fluorescence microscopy and waterborne treatment with isoniazid was commenced at external concentrations of 0, 3.75, 7.5, 15, 30, and 75 mg/L corresponding to 0, 0.25, 0.5, 1, 2, and 5x MIC. Quantification of the bacterial burden was repeated within individual larva at 3 dpi and 4 dpi to assess individual early bactericidal activity. Internal isoniazid exposure was quantified by LC-MS/MS of whole zebrafish larval homogenate samples as well as in larval blood samples in a parallel experiment with uninfected larvae treated with external isoniazid concentrations of 7.5, 15, 30, 75, and 150 mg/L corresponding to 0.5, 1, 2, 5, and 10x MIC. Figure 10.1 shows a schematic overview of the study design.

*10.6.2 Chemicals*

Isoniazid was acquired from Sigma-Aldrich (Sigma-Aldrich Chemie GmbH, Schnelldorf, Germany) and isoniazid-D4 internal standard from Santa Cruz (Santa Cruz Biotechnology, Santa Cruz, USA). Ethyl 3-aminobenzoate (tricaine) was purchased from Sigma-Aldrich. Cinnamaldehyde was acquired from Sigma-Aldrich. Nanopure water was used from a PURELAB water purification system (Veolia Water Technologies B.V., Ede, The Netherlands) unless otherwise stated. ULC-MS-grade methanol as well as ULC-MS-grade acetonitrile, LC-MS-grade water, and formic acid was acquired from Biosolve (Biosolve B.V., Valkenswaard, The Netherlands). Difco Middlebrook 7H10 agar and 7H9 medium, oleic acid-albumin-dextrose-catalase (OADC), and acid-albumin-dextrose-catalase (ADC) was acquired from BD (BD Biosciences, Sparks, USA). Polyvinylpyrrolidone-40 solution (PVP40) was acquired from Sigma-Aldrich.

*10.6.3 Zebrafish husbandry*

Zebrafish were maintained and handled following international consensus protocols[58]. Planning and execution of all experiments complied with European regulation[59]. Adult wild type VUmc zebrafish were kept in glass aquaria (max 6/L, volume 10L, 120x220x490 mm, Fleuren & Nooijen BV, Nederweert, The Netherlands) with circulating water (27.7°C ± 0.1 on a 14h/10h light/dark cycle, lights on at 08:00). Adult zebrafish were fed twice daily with artemia or feed particles (Gemma Micro/Diamond, Skretting, Nutreco NV, Amersfoort, The Netherlands). JUMO Acquis touch S (JUMO GmbH & Co, Weesp, The Netherlands) was used to control water quality.

Adult zebrafish were set-up for breeding overnight and in the morning at lights-on, separators between males and females were removed and fertilized eggs were collected within 30 minutes of fertilization.

Eggs, embryos, and larvae were kept in embryo medium (60 µg/mL Instant Ocean sea salts (Sera, Heinsberg, Germany) in demineralized water, daily refreshed) at 28°C, except for the treatment duration, when larvae were kept in treatment solution at 28°C until imaging or sampling.

*10.6.4 Internal exposure of isoniazid in zebrafish larvae*

Internal exposure of isoniazid in zebrafish larvae was quantified in larval homogenates and blood samples after waterborne treatment with isoniazid concentrations at external concentrations of 0.5, 1, 2, 5, and 10x MIC (7.5, 15, 30, 75, and 150 mg/L).

Homogenate samples were taken with at least three replicates of 5 larvae at time points 0.25, 0.5, 1, 2, 3, 6, 8, 9, 18, 20, 22, 24, 26, 32, 42, 44, 46, 48, and 50 hours after start of treatment. Zebrafish larvae were washed 4 times with 20/80 methanol/water (v/v) using Netwell inserts (Corning Life Sciences B.V., Amsterdam, The Netherlands) and transferred to Safe-Lock tubes (Eppendorf Nederland B.V., Nijmegen, The Netherlands). Excess volume was removed and 50 µL of 200 ng/mL isoniazid-D4 internal standard was added after which the samples were snap-frozen in liquid nitrogen and stored at-80°C until quantification.

Blood samples were taken after 48 hours of treatment at the highest external concentration of 150 mg/L to ascertain quantifiable levels, using a previously published method[38]. In short, zebrafish larvae of 5 dpf were washed 4 times as described above, superficially dried, and transferred to an agarose microscopy slide, after which a pulled needle (0.75 mm borosilicate class capillary without filament, Sutter Instruments, Novato, California, USA) positioned in a micromanipulator (World Precision Instruments, Berlin, Germany) attached to a CellTram Vario oil pump (Eppendorf) was used to sample the blood from the posterior cardinal vein under 20x magnification (Leica, Amsterdam, The Netherlands). An image of each blood sample was captured to calculate blood volume before the sample was injected into a 2 µL heparin droplet (5 International Units/mL) and pooled (19-32 blood samples per replicate) into a 0.5 mL tube (Eppendorf). Blood samples were kept at-80°C until quantification.

*10.6.5 Quantification of isoniazid in homogenate and blood samples*

Isoniazid was quantified by LC-MS/MS. Derivatization with cinnamaldehyde was performed to achieve adequate retention for LC separation.

Samples of whole zebrafish larva were thawed and 100 µL methanol and 100 µL of 0.5 mm zirconium oxide bullets (NextAdvance, New York, USA) were added. The samples were homogenized using a Bullet Blender (NextAdvance) for at least two rounds of 5 minutes at speed 5. Extraction and derivatization was performed by adding 800 µL acetonitrile, 100 µL 1% cinnamaldehyde in methanol, and 100 µL formic acid and shaking for 20 minutes at 650 rpm (IKA, Staufen im Breisgau, Germany). Samples were centrifuged for 10 minutes at 20,000g, 90% was transferred to a new Safe-Lock tube, and evaporated until dryness in a Labconco vacuum centrifuge (Beun de Ronde, Abcoude, The Netherlands). The residue was reconstituted into 200 µL methanol, centrifuged for 10 minutes at 20,000g and the supernatant was transferred to an LC-MS/MS vial with a glass insert for 5 µL injection into the LC-MS/MS. Quality control (QC) and calibration curve samples were prepared by spiking blank homogenate samples. The QC samples were prepared at the levels of 4, 125, and 225 ng/mL. The calibration curve samples were prepared at the levels of 0, 2, 5, 10, 25, 50, 100, 150, and 250 ng/mL. Blood samples were thawed and briefly centrifuged to concentrate the small sample into the bottom of the tube. 2.5 µL of 200 ng/mL internal standard solution was added. Extraction and derivatization was performed by addition of 200 µL acetonitrile and 50 µL methanol, and 25 µL 1% cinnamaldehyde in methanol and 25 µL formic acid, and samples were shaken for 20 minutes at 650 rpm. Samples were evaporated until dry, reconstituted in 10 µL methanol, and centrifuged for 10 minutes at 20,000 g, after which they were transferred to an LC-MS/MS vial with a glass insert upon 5 µL injection into the LC-MS/MS. An academic calibration curve in methanol was prepared with concentrations 0, 2, 3, 5, 8, 10, 25, 50, 100, 150, and 250 ng/mL.

Quantification of isoniazid was performed on an ultra high-performance liquid chromatography (UHPLC) system (Shimadzu Nexera X2, 's Hertogenbosch, The Netherlands) with a triple quadrupole mass spectrometry (MS) detector (TSQ Vantage, Thermo Fisher Scientific, Breda, The Netherlands). Electron Spray Ionization in positive modes was used to obtain derivative ions.

Chromatography was performed at a flow of 0.4 mL/min on a Luna Omega Polar C18 1.7 µm 100x2.1mm column with a 5 mm guard column with the same packing material (Phenomenex, Utrecht, The Netherlands). The temperature of the column was maintained at 40°C. Gradient elution was performed with two UHPLC pumps using methanol/water mixtures with 0.01% formic acid. The gradient started at the time of injection and increased from a 49/51 methanol/water v/v ratio to a 72/28 methanol/water v/v ratio within 4 minutes. The column was flushed with 95/5 methanol/water v/v ratio starting at 4.1 minutes for 2.4 minutes after which the system was equilibrated to initial conditions.

Within the MS system, the vaporizer temperature was set at 300°C and capillary temperature at 250°C. Sheath gas pressure was 40 psi, Multiple Reaction Monitoring was used to quantify isoniazid-derivative (MH+ = 252.1 m/z) and isoniazid-D4-adduct (MH+ = 256.1 m/z). For isoniazid-derivative, the fragments were 79.01, and 121.01 m/z and for the internal standard-derivative the fragments were 83.10, and 124.96 m/z. The sheath gas pressure was 40 psi, auxiliary gas pressure was 15 psi, S lens RF amplitude was 63 V, capillary pressure was 1.190 mTorr. Detection limit was 0.5 ng/mL, and lower limit of quantification (LLOQ) was 1.75 ng/mL. The LC-MS/MS method was validated according to the US Food and Drug Administration guidelines[60]. LC-Quan software (v. 2.7, Thermo Fisher Scientific) was used for data acquisition where isoniazid peak area was corrected by internal standard peak area, and calibration was performed with weighted linear regression using 1/y as weighting factor. Of the pharmacokinetic data points, 3% was below the LLOQ and 1% was above the highest calibration standard, these samples were excluded from the analysis[61].

*10.6.6 Bacterial strain preparation*

The bacterial strain *M. marinum* E11 expressing mCherry fluorescent protein[62] was used to induce an infection in zebrafish embryos. *M. marinum* E11 was cultured and harvested as previous described[63]. In short, a colony of *M. marinum* E11 was picked from 7H10 supplemented with 10% OADC, the colony was suspended in 7H9 supplemented with 10% ADC, and cultured overnight at 28°C. The optical density at 600 nm ($OD_{600}$) of bacteria was measured the next day (Eppendorf Biophotometer 6131, Eppendorf, Hamburg, Germany). The logarithmic phase bacteria were harvested and washed 3 times with sterile phosphate buffer saline (PBS). The infection inoculum was resuspended to a target concentration of 200 CFU/nL in 2% PVP40. The MIC of the used strain had been determined to be 15 mg/L, in line with reported values[42].

*10.6.7* M. marinum *bacterial burden in zebrafish larvae upon isoniazid treatment*

The injection procedure was performed as described previously[63]. In short, at 24 hpf zebrafish embryos were dechorionated manually with fine tweezers (F6521-1E Jewelers forceps Dumont No. 5, Sigma-Aldrich). The microinjection needles (BF100-75-10, Sutter Instruments) were prepared with a micropipette puller device (P-97 Flaming/Brown Micropipette Puller, Sutter Instrument). Embryos of 28 hpf were anaesthetized with 200 µg/mL tricaine 10 minutes prior to injection and injected with 1 nL of 200 CFU/nL *M. marinum* E11 using the microinjection system (FemtoJet, Eppendorf, Hamburg, Germany), into the caudal vein at the blood island. After injection, the injected embryos were kept at 28°C. To quantify the established infection at 2 dpi, a Fluorescence Stereo Microscope (Leica MZ16FA, Leica Microsystems, Wetzlar, Germany) equipped with digital camera (Leica DFC420 C, Leica Microsystems) was utilized for fluorescence imaging, after which the larvae were transferred to 96 well plates (655180, Greiner Bio-One, Kremsmünster, Austria) with isoniazid solutions of 0, 3.75, 7.5, 15, 30, or 75 mg/L in embryo medium with at least n = 20 per group. At 3 and 4 dpi, fluorescence imaging of individual larvae was repeated after which they were transferred to a new 96 well plate with fresh isoniazid treatment solution (3 dpi) or sacrificed (4 dpi).

Automated image analysis was performed as reported before[19,27], where count of pixels with fluorescence is assumed to correlate directly with the bacterial burden. Potential differences in the bacterial burden between larvae at the start of treatment were tested by non-parametric Kruskal-Wallis test. 12.7% (16/126) of the larvae were removed from the dataset due to improper injection, developmental defects (e.g. cardiac edema), or death due to mechanical damage from handling or otherwise.

*10.6.8 Quantification of the exposure-response relationship for isoniazid in zebrafish larvae*

A pharmacokinetic-pharmacodynamic model was developed to quantify the internal exposure-response relationship of isoniazid on bacterial growth. NONMEM (version 7.3)[64] through interfaces Pirana (version 2.9.6)[65] and PsN (version 4.7.0)[66] was used for non-linear mixed effects modelling. R (version 3.5.0)[67] through the Rstudio interface (version 1.1.383, RStudio Inc, Boston, Massachusetts, USA) was used for data transformation and graphical output. The First Order Conditional Estimation (FOCE) algorithm with interaction is used for pharmacokinetic-pharmacodynamic modelling.

In the pharmacokinetic component of the model, the homogenate and blood sample data were fitted simultaneously. The treatment medium was represented as depot compartment from which a first order absorption rate constant into a one compartment model with distribution volume and linear or non-linear (Michaelis-Menten) elimination was estimated. Concentration in the treatment medium was assumed to be constant, as supported by measurements of concentrations (Supplementary Figure S10.4). Age was tested as covariate (predictor) on absorption and elimination rate constants using a linear, power or exponential relationship, in addition to a discrete increase in absorption rate constant between 3 and 4 dpf to reflect the impact of the opening of the gastro-intestinal (GI) tract[28]. Out of additive, proportional, or a combination error models, the residual error, describing biological and experimental error, was best described by a combination of an additive and proportional error model for the isoniazid amounts in homogenates and a proportional error model for isoniazid concentrations in the blood samples. A visual predictive check of the pharmacokinetic component of the model was performed using 500 simulations, stratified per dose.

The pharmacodynamic component of the model was fitted through $\log_{10}$ transformed data of the bacterial burden. Bacterial growth was tested using exponential (Equation 2), Gompertz (Equation 3), or logistic (Equation 4) growth functions.

$$\frac{\mathrm{dBac}}{\mathrm{dt}} = \mathrm{k_g} \cdot \mathrm{Bac} \tag{2}$$

$$\frac{\mathrm{dBac}}{\mathrm{dt}} = \mathrm{k_g} \cdot \log\left(\frac{\mathrm{B_{max}}}{\mathrm{Bac}}\right) \tag{3}$$

$$\frac{\mathrm{dBac}}{\mathrm{dt}} = \mathrm{k_g} \cdot \log(\mathrm{B_{max}} - \mathrm{Bac}) \tag{4}$$

in which Bac represented the bacterial burden, t time (h), $k_g$ the growth rate ($h^{-1}$), and $B_{max}$ the maximum capacity of the system ($\log_{10}$ fluorescence). Because no ceiling of bacterial growth was observed in the data, the maximum capacity of the system could not be estimated for the Gompertz or logistic growth function. Growth and decay cannot be estimated separately as this is mathematically not identifiable given the data. Therefore a net effect was estimated for growth, with implications on its interpretation, i.e. a negative growth meant decay or kill.

Based on the blood sample and homogenate data at 5 dpf, the distribution volume at this age was estimated. This distribution volume was subsequently scaled to 3 and 4 dpf based on total larval volume[68]. The pharmacokinetic component of the model converts total isoniazid amounts from homogenates to concentrations using these distribution volumes (Equation 5).

$$C_{INH} = \frac{A_{INH}}{V_d} \quad (5)$$

in which $C_{INH}$ is the concentration of isoniazid (pmole/µL or µmole/L (µM)), $A_{INH}$ is the amount of isoniazid (pmole) in the homogenate samples, and $V_d$ is the scaled volume of distribution (µL).
For the exposure-response relationship (EFF), linear (Equation 6), Emax (Equation 7), or sigmoidal Emax (Equation 8) functions were tested.

$$EFF = SLP \cdot C_{INH} \quad (6)$$

$$EFF = \frac{E_{max} \cdot C_{INH}}{EC_{50} + C_{INH}} \quad (7)$$

$$EFF = \frac{E_{max} \cdot C_{INH}^{\gamma}}{EC_{50}^{\gamma} + C_{INH}^{\gamma}} \quad (8)$$

in which SLP represents the slope ($\mu M^{-1}$), $E_{max}$ the maximal response (-), $EC_{50}$ the concentration of isoniazid responsible for 50% of the maximal response (µM), and γ the Hill exponent (-).

The exposure-response relationship was linked to the bacterial burden as either inhibition of growth or as kill term as shown for the exponential growth function as example in Equation 9 and Equation 10, respectively.

$$\frac{dBac}{dt} = k_g \cdot Bac \cdot (1 - EFF) \quad (9)$$

$$\frac{dBac}{dt} = k_g \cdot Bac - EFF \cdot Bac \quad (10)$$

Inter-individual variability was tested on the estimate of the inoculum, as well as for the parameters of the exposure-response relationship, and reported as coefficient of variation[69]. Out of an additive, proportional, or a combination of additive and proportional error models, a proportional error model, parameterized as an additive error on the $\log_{10}$ transformed data, best described the residual variability in the bacterial burden.

Model selection was performed based on the likelihood ratio test between nested models, in which a drop in objective function value of 3.84 corresponded to $p < 0.05$ between models with a single degree of freedom difference, assuming a $\chi^2$-distribution. Physiologic plausibility of parameter estimates, as well as visual assessment of goodness-of-fit plots[70] were also used for model selection. Precision of structural parameters was considered to be acceptable when relative standard errors of the structural parameters remained below 50%.

*10.6.9 Translation of isoniazid response to humans*
To quantitatively compare the findings for isoniazid response in zebrafish infected with *M. marinum* to findings in humans infected with *M. tuberculosis*, the exposure-response relationship obtained in the zebrafish larvae was translated to humans as a proof-of-concept. For this, first the isoniazid concentration-time profile in humans was simulated. The concentration-time profile in humans was simulated from a previously published pharmacokinetic model[33], for a period of 7 days of isoniazid oral dosing at 150, 300, and 450 mg for 1,000 individuals per dose group with a ratio of fast and slow metabolizing of 50:50.

Second, the simulated concentrations for the 1,000 individuals per dose group were linked to the exposure-response relationship for *M. marinum* in zebrafish larvae quantified here, to predict the isoniazid response on the bacterial burden. Two translational factors were utilized[31]. The difference in sensitivity to isoniazid was taken into account by using the ratio of the MIC for *M. marinum* and *M. tuberculosis*[49]. The difference in infection stage between the zebrafish, which is in logarithmic phase, and the patients, which are assumed to be in stationary phase (150 days of infection)[31], was taken into account by scaling the isoniazid drug response as quantified previously[51]. From the multistate tuberculosis pharmacometric model, it is clear that the majority of the mycobacteria are in the fast-multiplying state in the logarithmic phase, while they are in the slow- and non-multiplying state in the stationary phase[50]. The ratio of maximum isoniazid-induced kill rates on the fast- and slow-multiplying state (no effect of isoniazid was observed or quantified on the non-multiplying state) is utilized as translational factor to account for the difference in infection stage[51].

Third, the obtained isoniazid response was quantitatively compared to published bacterial burden data in humans[34–36]. Inoculum of the simulation was set at the mean of the reported inoculi[34–36], and exponential growth rate of the bacterial burden was assumed to be similar irrespective of measurement by fluorescence or CFU/mL.

## 10.7 Acknowledgments

The authors thank Parth Upadhyay for code-review of the R- and NONMEM-scripts, and Astrid M. van der Sar for sharing the wild type VUmc zebrafish line.

## 10.8 Data availability statement

Final model codes and datasets are publicly available through the DDMoRe Repository, Model ID DDMODEL00000311 (http://repository.ddmore.foundation/model/DDMODEL00000311).

## 10.9 References

1. Furin J, Cox H, Pai M. Tuberculosis. Lancet. 2019;393(10181):1642-1656.
2. General Assembly of the United Nations. Transforming our world: The 2030 Agenda for Sustainable Development. Gen Assem 70th Sess. 2015;A/RES/70/1.
3. United Nations. The sustainable development goals report 2019. United Nations Publ issued by Dep Econ Soc Aff. 2019.
4. DiMasi JA, Grabowski HG, Hansen RW. Innovation in the pharmaceutical industry: New estimates of R&D costs. J Health Econ. 2016;47:20-33.
5. World Health Organization. Tuberculosis laboratory biosafety manual. World Heal Organ Publ ISBN 978 92 41504638. 2012:1-60.
6. Ginsberg AM, Spigelman M. Challenges in tuberculosis drug research and development. Nat Med. 2007;13(3):290-294.
7. Lienhardt C, Glaziou P, Uplekar M, et al. Global tuberculosis control: lessons learnt and future prospects. Nat Rev Microbiol. 2012;10:407-416.
8. Koul A, Arnoult E, Lounis N, et al. The challenge of new drug discovery for tuberculosis. Nature. 2011;469:483-490.
9. Schulthess P, Van Wijk RC, Krekels EHJ, et al. Outside-in systems pharmacology combines innovative computational methods with high-throughput whole vertebrate studies. CPT Pharmacometrics Syst Pharmacol. 2018;7:285-287.
10. Rennekamp AJ, Peterson RT. 15 years of zebrafish chemical screening. Curr Opin Chem Biol. 2015;24:58-70.
11. Van Wijk RC, Krekels EHJ, Hankemeier T, et al. Systems pharmacology of hepatic metabolism in

zebrafish larvae. Drug Discov Today Dis Model. 2016;22:27-34.
12. Meijer AH, Spaink HP. Host-pathogen interactions made transparent with the zebrafish model. Curr Drug Targets. 2011;12(7):1000-1017.
13. Meijer AH. Protection and pathology in TB: Learning from the zebrafish model. Semin Immunopathol. 2016;38:261-273.
14. Tobin DM, May RC, Wheeler RT. Zebrafish: A see-through host and a fluorescent toolbox to probe host–pathogen interaction. PLoS Pathog. 2012;8(1):e1002349.
15. Myllymäki H, Bäuerlein CA, Rämet M. The zebrafish breathes new life into the study of tuberculosis. Front Immunol. 2016;7(MAY).
16. Carvalho R, De Sonneville J, Stockhammer OW, et al. A high-throughput screen for tuberculosis progression. PLoS One. 2011;6(2):1-8.
17. Ordas A, Raterink R-J, Cunningham F, et al. Testing tuberculosis drug efficacy in a zebrafish high-throughput translational medicine screen. Antimicrob Agents Chemother. 2015;59(2):753-762.
18. Tobin DM, Ramakrishnan L. Comparative pathogenesis of Mycobacterium marinum and Mycobacterium tuberculosis. Cell Microbiol. 2008;10(5):1027-1039.
19. Stoop EJM, Schipper T, Rosendahl Huber SK, et al. Zebrafish embryo screen for mycobacterial genes involved in the initiation of granuloma formation reveals a newly identified ESX-1 component. Dis Model Mech. 2011;4(4):526-536.
20. Bussi C, Gutierrez MG. Mycobacterium tuberculosis infection of host cells in space and time. FEMS Microbiol Rev. 2019;43:341-361.
21. Kolibab K, Yang A, Parra M, et al. Time to detection of Mycobacterium tuberculosis using the MGIT 320 system correlates with colony counting in preclinical testing of new vaccines. Clin Vaccine Immunol. 2014;21(3):453-455.
22. Kumar N, Vishwas KG, Kumar M, et al. Pharmacokinetics and dose response of anti-TB drugs in rat infection model of tuberculosis. Tuberculosis. 2014;94(3):282-286.
23. Jayaram R, Shandil RK, Gaonkar S, et al. Isoniazid pharmacokinetics-pharmacodynamics in an aerosol infection model of tuberculosis. Antimicrob Agents Chemother. 2004;48(8):2951-2957.
24. Bartelink I, Zhang N, Keizer R, et al. New paradigm for translational modeling to predict long-term tuberculosis treatment response. Clin Transl Sci. 2017;(May):366-379.
25. Morgan P, Van der Graaf PH, Arrowsmith J, et al. Can the flow of medicines be improved? Fundamental pharmacokinetic and pharmacological principles toward improving Phase II survival. Drug Discov Today. 2012;17(9/10):419-424.
26. Jindani A, Aber VR, Edwards EA, et al. The early bactericidal activity of drugs in patients with pulmonary tuberculosis. Am Rev Respir Dis. 1980;121(6):939-949.
27. Nezhinsky A, Verbeek FJ. Pattern recognition for high throughput zebrafish imaging using genetic algorithm optimization. In: Dijkstra T, Tsivtsivadze E, Heskes T, Marchiori E, eds. Lecture Notes in Bioinformatics 6282. Berlin- Heidelberg: Springer-Verlag; 2010:301-312.
28. Van Wijk RC, Krekels EHJ, Kantae V, et al. Impact of post-hatching maturation on the pharmacokinetics of exogenous compounds in zebrafish larvae. Sci Rep. 2018;9:2149.
29. Ng ANY, De Jong-Curtain TA, Mawdsley DJ, et al. Formation of the digestive system in zebrafish: III. Intestinal epithelium morphogenesis. Dev Biol. 2005;286(1):114-135.
30. Musuamba F, Manolis E, Holford N, et al. Advanced methods for dose and regimen finding during drug development: summary of the EMA/EFPIA workshop on dose finding (London 4-5 December 2014). CPT Pharmacometrics Syst Pharmacol. 2017;6:418-429.
31. Wicha SG, Clewe O, Svensson RJ, et al. Forecasting clinical dose-response from preclinical studies in tuberculosis research: translational predictions with rifampicin. Clin Pharmacol Ther. 2018;104(6):1208-1218.
32. De Groote MA, Gilliland JC, Wells CL, et al. Comparative studies evaluating mouse models used for efficacy testing of experimental drugs against Mycobacterium tuberculosis. Antimicrob Agents Chemother. 2011;55(3):1237-1247.
33. Wilkins JJ, Langdon G, McIlleron H, et al. Variability in the population pharmacokinetics of isoniazid

in South African tuberculosis patients. Br J Clin Pharmacol. 2011;72(1):51-62.
34. Li L, Mahan CS, Palaci M, et al. Sputum Mycobacterium tuberculosis mRNA as a marker of bacteriologic clearance in response to antituberculosis therapy. J Clin Microbiol. 2010;48(1):46-51.
35. Johnson JL, Hadad DJ, Boom WH, et al. Early and extended early bactericidal activity of levofloxacin, gatifloxacin and moxifloxacin in pulmonary tuberculosis. Int J Tuberc Lung Dis. 2006;10(6):605-612.
36. Hafner R, Cohn JA, Wright DJ, et al. Early bactericidal activity of isoniazid in pulmonary tuberculosis: Optimization of methodology. Am J Respir Crit Care Med. 1997;156(3 I):918-923.
37. Kantae V, Krekels EHJ, Ordas A, et al. Pharmacokinetic modeling of paracetamol uptake and clearance in zebrafish larvae: Expanding the allometric scale in vertebrates with five orders of magnitude. Zebrafish. 2016;13(6):504-510.
38. Van Wijk RC, Krekels EHJ, Kantae V, et al. Mechanistic and quantitative understanding of pharmacokinetics in zebrafish larvae through nanoscale blood sampling and metabolite modelling of paracetamol. J Pharmacol Exp Ther. 2019;371:15-24.
39. Spaink HP, Cui C, Wiweger MI, et al. Robotic injection of zebrafish embryos for high-throughput screening in disease models. Methods. 2013;62(3):246-254.
40. Gillespie SH, Gosling RD, Charalambous BM. A reitrerative method for calculating the early bactericidal activity of antituberculosis drugs. Am J Respir Crit Care Med. 2002;166(1):31-35.
41. Greenwood DJ, Dos Santos MS, Huang S, et al. Subcellular antibiotic visualization reveals a dynamic drug reservoir in infected macrophages. Science. 2019;364(6447):1279-1282.
42. Aubry A, Jarlier V, Escolano S, et al. Antibiotic susceptibility pattern of Mycobacterium marinum. Antimicrob Agents Chemother. 2000;44(11):3133-3136.
43. Weerakhun S, Hatai K, Murase T, et al. In vitro and in vivo activities of drugs against Mycobacterium marinum in yellowtail Seriola quinqueradiata. Fish Pathol. 2008;43(3):106-111.
44. Boot M, Sparrius M, Jim KK, et al. iniBAC induction is vitamin B12- and MutAB-dependent in mycobacterium marinum. J Biol Chem. 2016;291(38):19800-19812.
45. Boot M, Jim KK, Liu T, et al. A fluorescence-based reporter for monitoring expression of mycobacterial cytochrome bd in response to antibacterials and during infection. Sci Rep. 2017;7(1):1-10.
46. Gumbo T, Louie A, Liu W, et al. Isoniazid bactericidal activity and resistance emergence: Integrating pharmacodynamics and pharmacogenomics to predict efficacy in different ethnic populations. Antimicrob Agents Chemother. 2007;51(7):2329-2336.
47. Budha NR, Lee RB, Hurdle JG, et al. A simple in vitro PK/PD model system to determine time-kill curves of drugs against Mycobacteria. Tuberculosis. 2009;89:378-385.
48. Hemanth Kumar AK, Kannan T, Chandrasekaran V, et al. Pharmacokinetics of thrice-weekly rifampicin, isoniazid and pyrazinamide in adult tuberculosis patients in India. Int J Tuberc Lung Dis. 2016;20(9):1236-1241.
49. Schön T, Juréen P, Giske CG, et al. Evaluation of wild-type MIC distributions as a tool for determination of clinical breakpoints for Mycobacterium tuberculosis. J Antimicrob Chemother. 2009;64(4):786-793.
50. Clewe O, Aulin L, Hu Y, et al. A multistate tuberculosis pharmacometric model: A framework for studying anti-tubercular drug effects in vitro. J Antimicrob Chemother. 2016;71(4):964-974.
51. Clewe O, Wicha SG, de Vogel CP, et al. A model-informed preclinical approach for prediction of clinical pharmacodynamic interactions of anti-TB drug combinations. J Antimicrob Chemother. 2018;73(2):437-447.
52. Chen C, Ortega F, Rullas J, et al. The multistate tuberculosis pharmacometric model: a semi-mechanistic pharmacokinetic-pharmacodynamic model for studying drug effects in an acute tuberculosis mouse model. J Pharmacokinet Pharmacodyn. 2017;44(2):133-141.
53. Chen C, Wicha SG, De Knegt GJ, et al. Assessing pharmacodynamic interactions in mice using the multistate tuberculosis pharmacometric and general pharmacodynamic interaction models. CPT Pharmacometrics Syst Pharmacol. 2017;6(11):787-797.
54. Svensson RJ, Simonsson USH. Application of the multistate tuberculosis pharmacometric model in patients with rifampicin-treated pulmonary tuberculosis. CPT Pharmacometrics Syst Pharmacol.

2016;5(5):264-273.
55. Van Wijk RC, Van der Sar AM, Krekels EHJ, et al. Quantification of natural growth of two strains of Mycobacterium marinum for translational anti-tuberculosis drug development. Submitted. 2019.
56. Jindani A, Doré CJ, Mitchison DA. Bactericidal and sterilizing activities of antituberculosis drugs during the first 14 days. Am J Respir Crit Care Med. 2003;167(10):1348-1354.
57. Strähle U, Scholz S, Geisler R, et al. Zebrafish embryos as an alternative to animal experiments — A commentary on the definition of the onset of protected life stages in animal welfare regulations. Reprod Toxicol. 2012;33:128-132.
58. Westerfield M. The zebrafish book. A guide for the laboratory use of zebrafish (Danio rerio). 4th ed. Eugene, OR, USA: University of Oregon Press; 2000.
59. EU. Council Directive 2010/63/EU on the protection of animals used for scientific purposes. Off J Eur Union. 2010;L276/33.
60. US Food and Drug Administration. Bioanalytical method validation guidance for industry. FDA. 2018:May.
61. Beal SL. Ways to fit a PK model with some data below the quantification limit. J Pharmacokinet Pharmacodyn. 2001;28(5):481-504.
62. Van der Sar AM, Spaink HP, Zakrzewska A, et al. Specificity of the zebrafish host transcriptome response to acute and chronic mycobacterial infection and the role of innate and adaptive immune components. Mol Immunol. 2009;46(11-12):2317-2332.
63. Benard EL, Van der Sar AM, Ellett F, et al. Infection of zebrafish embryos with intracellular bacterial pathogens. J Vis Exp. 2012;61:e3781.
64. Beal S, Sheiner L, Boeckmann A, et al. NONMEM 7.3.0 users guides. (1989-2013). ICON Development Solutions, Hanover, MD, USA.
65. Keizer R, Van Benten M, Beijnen J, et al. Pirana and PCluster: A modeling environment and cluster infrastructure for NONMEM. Comput Methods Programs Biomed. 2011;101(1):72-79.
66. Lindbom L, Pihlgren P, Jonsson E. PsNtoolkit — a collection of computer intensive statistical methods for non-linear mixed effect modeling using NONMEM. Comput Methods Programs Biomed. 2005;79(3):241-257.
67. R Core Team. R: A language and environment for statistical computing. R Found Stat Comput Vienna, Austria. 2014.
68. Guo Y, Veneman WJ, Spaink HP, et al. Three-dimensional reconstruction and measurements of zebrafish larvae from high-throughput axial-view in vivo imaging. Biomed Opt Express. 2017;8(5):2611-2634.
69. Mould DR, Upton RN. Basic concepts in population modeling, simulation, and model-based drug development-part 2: introduction to pharmacokinetic modeling methods. CPT pharmacometrics Syst Pharmacol. 2013;2(April):e38.
70. Nguyen THT, Mouksassi M-S, Holford N, et al. Model evaluation of continuous data pharmacometric models: metrics and graphics. CPT Pharmacometrics Syst Pharmacol. 2017;6:87-109.

## 10.10 Supplementary material

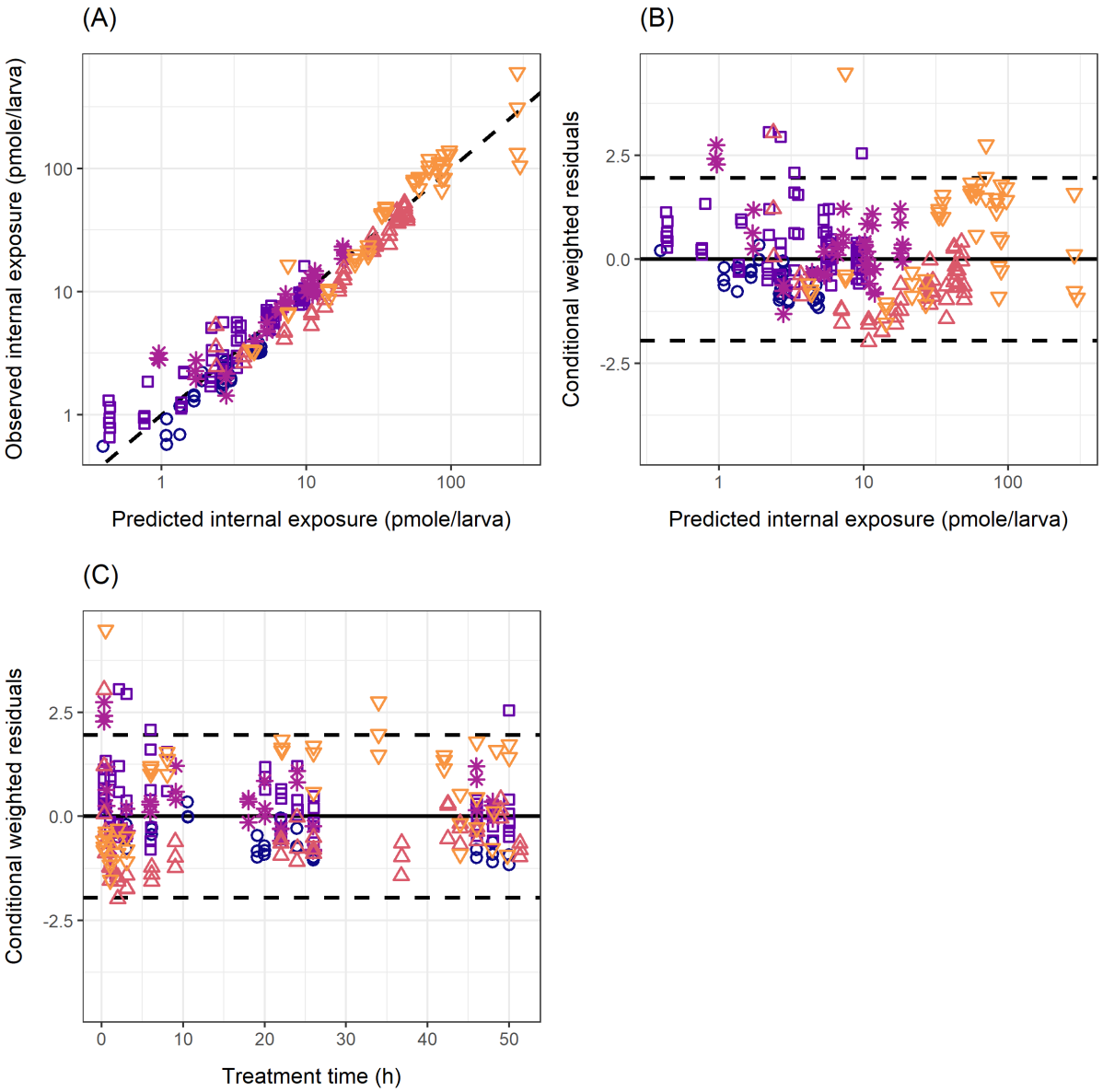


Supplementary Figure S10.1 Goodness-of-fit plots for the pharmacokinetic component of the final pharmacokinetic-pharmacodynamic model in zebrafish larvae. (a) Observed vs predicted, dotted line is the line of unity. (b) Conditional weighted residuals vs prediction, solid line represents zero, dashed lines represent 95% interval between ±1.96 standard deviation. (c) Conditional weighted residuals vs time, solid line represents zero, dashed lines represent 95% interval between ±1.96 standard deviation. Symbols represent waterborne isoniazid doses 0.5 (blue circle), 1 (purple square), 2 (lilac star), 5 (orange upward triangle) and 10 (yellow downward triangle) x MIC (MIC = 15 mg/L). Only small trends for different doses were observed which suggested only limited bias of predicted internal isoniazid amounts by the final model.

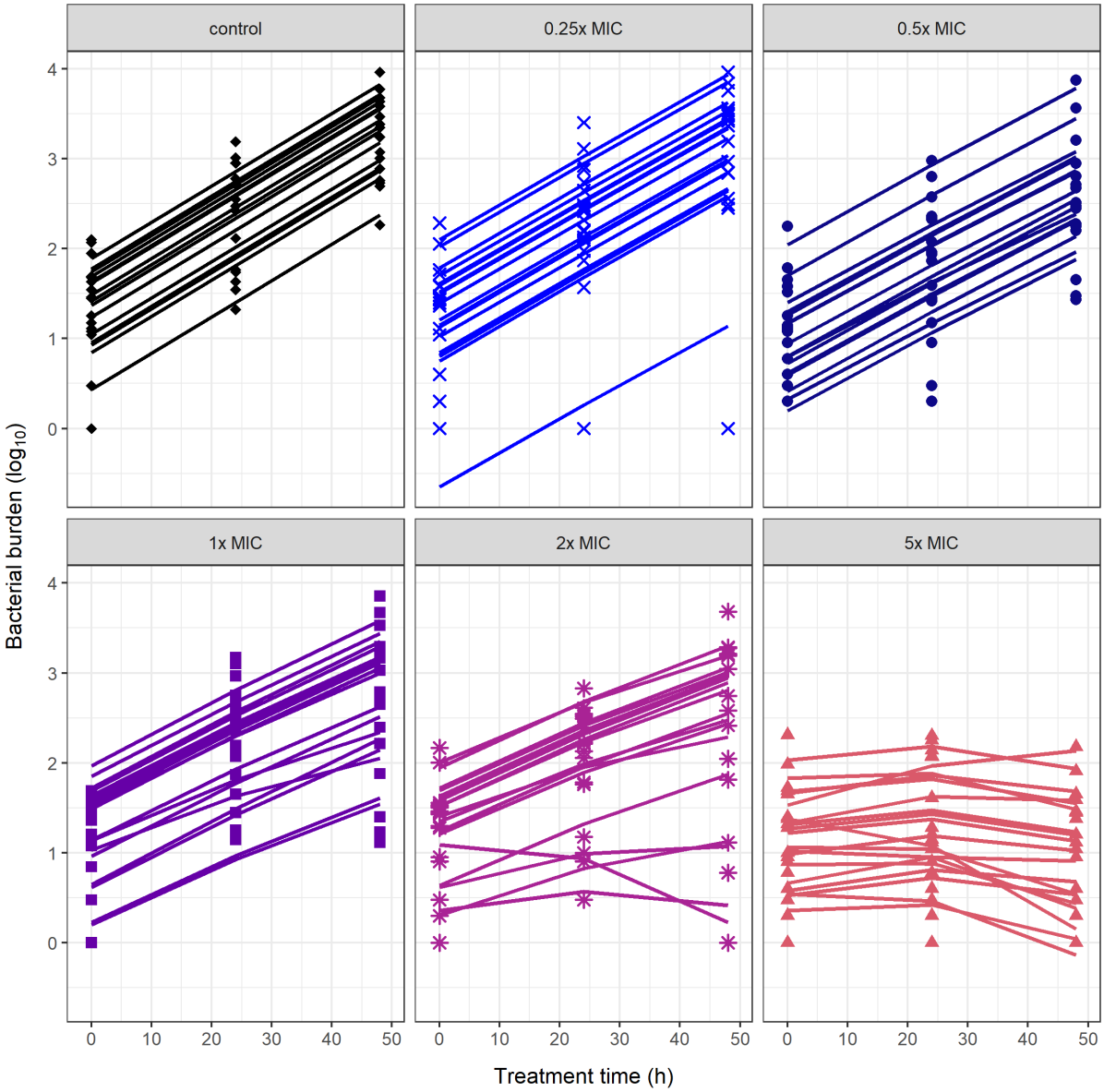


Supplementary Figure S10.2 Model-based individual prediction of the bacterial burden after isoniazid treatment in zebrafish larvae infected with *M. marinum*. The bacterial burden as $log_{10}$-transformed fluorescent pixel count is shown over treatment time of 50 hours at isoniazid doses in the external treatment medium of 0.25 (light blue crosses and line), 0.5 (blue circles and line), 1 (purple squares and line), 2 (lilac stars and line), and 5 (orange upward triangles and line) x MIC (MIC = 15 mg/L), in addition to control (black diamonds and line). Symbols represent observed data, lines represent model prediction for individual zebrafish.

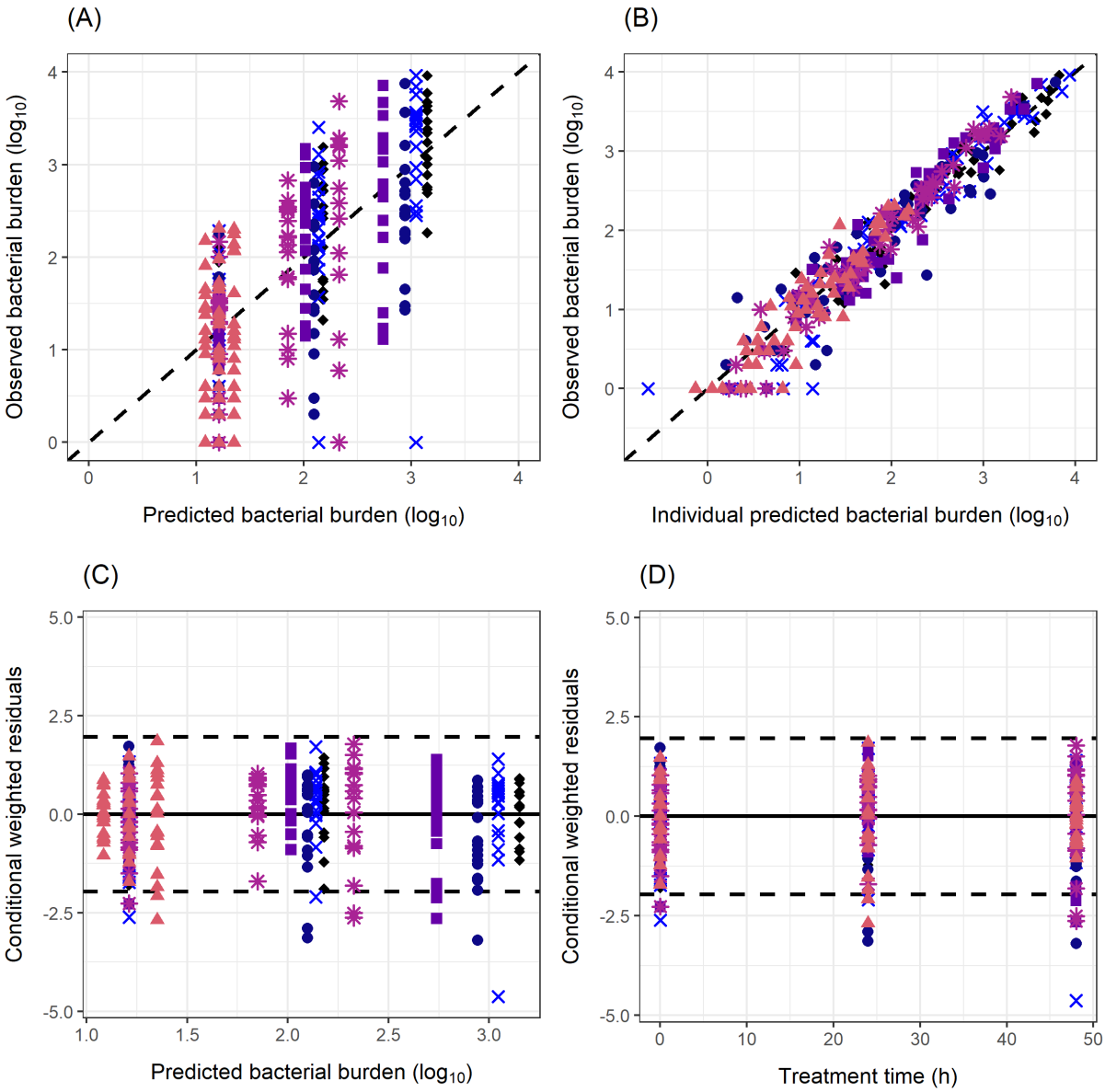


Supplementary Figure S10.3. Goodness-of-fit plots for pharmacodynamic component of the final pharmacokinetic-pharmacodynamic model in zebrafish. (a) Observed vs population predicted, dotted line is the line of unity. (b) Observed vs individual predicted, dotted line is the line of unity. (c) Conditional weighted residuals vs prediction, solid line represents zero, dashed lines represent 95% interval between ±1.96 standard deviation. (d) Conditional weighted residuals vs time, solid line represents zero, dashed lines represent 95% interval between ±1.96 standard deviation. Symbols represent doses 0 (black diamond), 0.25 (light blue cross), 0.5 (blue circle), 1 (purple square), 2 (lilac star), and 5 (orange upward triangle) x MIC (MIC = 15 mg/L). Lack of trends in the goodness-of-fit plots show no bias in the final model.

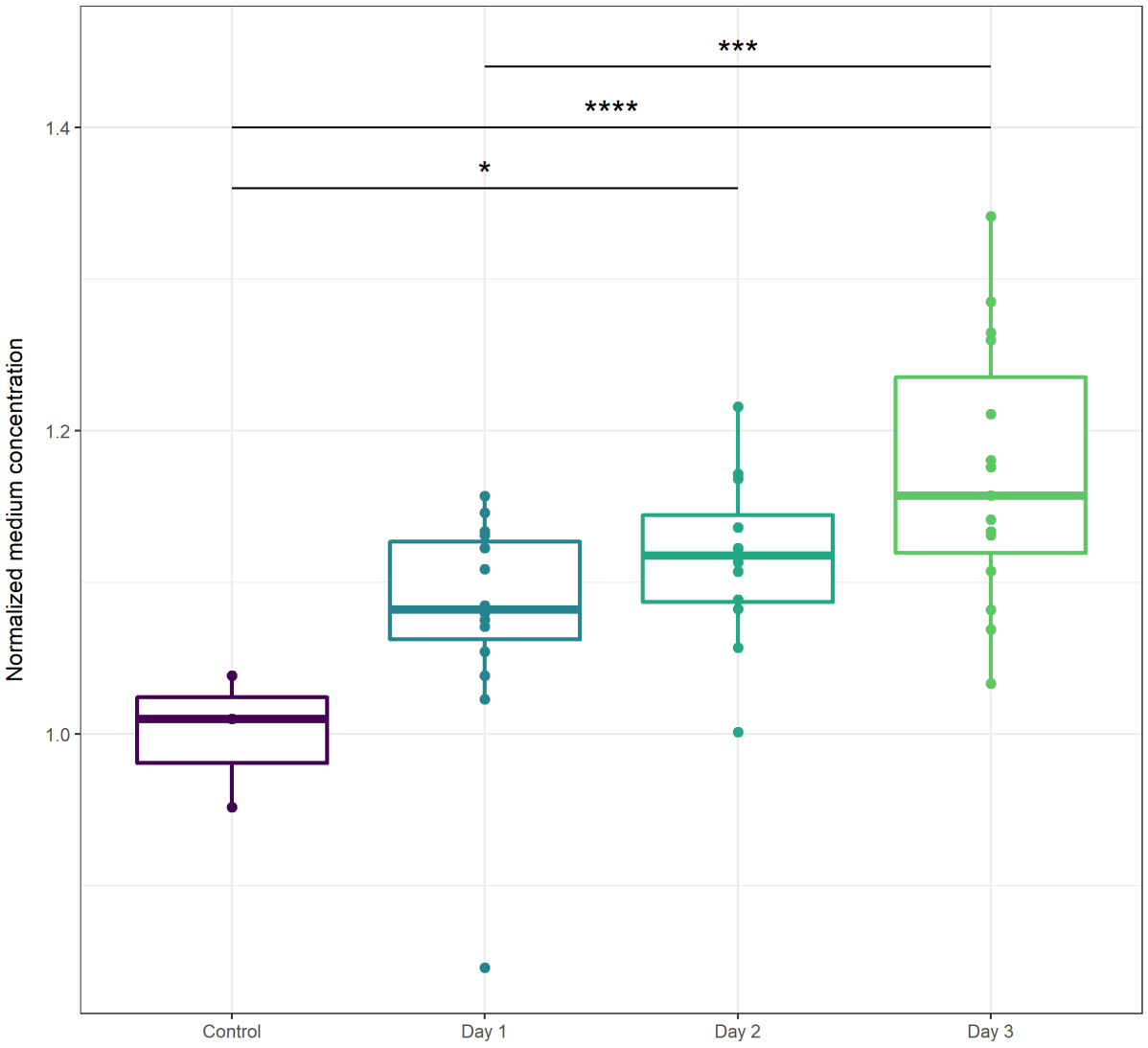


Supplementary Figure 10.4 Stability of waterborne isoniazid over treatment period. Concentrations were normalized to control. An increase of 10-15% was assumed to have negligible impact on the absorption from the treatment medium, which was therefore kept constant in the pharmacokinetic-pharmacodynamic model. Kruskal-Wallis with Dunn post hoc test: * $p < 0.05$, ** $p < 0.01$, *** $p < 0.005$, **** $p < 0.001$

## 10.11 NONMEM model code final pharmacokinetic-pharmacodynamic model

```
$PROBLEM PKPD
$INPUT ID TIME AMT DV EVID MDV CMT BQL AQL DOSE AGE AGE_H XEXP BLOOD FLAG
$DATA PKPD_dataset.csv IGNORE=@ IGNORE=(BQL.EQ.1) IGNORE=(AQL.EQ.1)

; time in hours of exposure
; amt in uM (concentration)
; DV in pmole / larvae or pmole / uL (uM) / log10(bac burden)
; Vd in uL
; AGE_H age in hpf

$SUBROUTINE ADVAN13 TOL=9

$MODEL
COMP ;CMT 1 dosing
COMP ;CMT 2 isoniazid in larva
COMP ;CMT 3 bacterial burden measured in log10(fluorescence pixels)

$PK

;-----PK-----

TVKE = THETA(1)          ;first order elimination rate
TVV2 = THETA(2)          ;distribution volume in uL/larva
TVKA = THETA(3) / 1e2    ;absorption at start of experiment
KA_GI = THETA(4)         ;effect of GI opening between 3 and 4 dpf on absorp-
tion
KA_HPF = THETA(5)        ;effect of age in hours post fertilization on ab-
sorption

;age effect on KA
KA = TVKA * KA_HPF**(AGE_H / 101)   ;median age is 101 hpf

;GI effect on KA
IF(AGE_H.LE.90) KIN = KA * DOSE
IF(AGE_H.GT.90) KIN = KA * DOSE * (1 + KA_GI)

KE = TVKE
V2 = TVV2

;-----PD-----

KG = THETA(6)                            ;exponential growth rate
INOC = THETA(7) * 1e1                    ;inoculum estimated
SLP = (THETA(8) / 1e2) * EXP(ETA(2))     ;slope (linear drug effect)

A_0(3) = INOC * EXP(ETA(1))              ;inoculum set as compartment ini-
tial value

$DES
DADT(1) = 0                              ;dosing compartment
DADT(2) = KIN - KE * A(2)                ;larva compartment isoniazid

;drug effect

;Distribution volume is estimated based on 5 dpf blood samples, but is ex-
pected to be lower with younger larvae of 3 and 4 dpf.
;It is here assumed that the distribution volume scales with total volume.

IF(AGE.EQ.3) THEN
```

```
V = V2 * 253/300          ;taking total volume into account (DOI: 10.1364/
BOE.8.002611)
ENDIF
IF(AGE.EQ.4) THEN
V = V2 * 263/300          ;taking total volume into account (DOI: 10.1364/
BOE.8.002611)
ENDIF
IF(AGE.EQ.5) THEN
V = V2                    ;taking total volume into account (DOI: 10.1364/
BOE.8.002611)
ENDIF

C = A(2)/V

EFF = 0                   ;for C is zero or NA
IF(C.GT.0) THEN
EFF = SLP * C
ENDIF

DADT(3) = KG * A(3) * (1 - EFF) ;bacterial burden (log10)

$ERROR

;-----PK-----

IF(FLAG.EQ.0.AND.BLOOD.EQ.0) THEN
IPRED = A(2)
Y = IPRED * (1 + EPS(1)) + EPS(2) ; comb error
W = SQRT(IPRED**2*SIGMA(1,1)**2    + SIGMA(2,2)**2)
IRES = DV - IPRED
ENDIF

IF(FLAG.EQ.0.AND.BLOOD.EQ.1) THEN
IPRED = A(2) / V2
Y = IPRED * (1 + EPS(3)) + EPS(4) ; comb error
W = SQRT(IPRED**2*SIGMA(3,3)**2    + SIGMA(4,4)**2)
IRES = DV - IPRED
ENDIF

;-----PD-----

IF(FLAG.EQ.1) THEN
IPRED = LOG10(A(3)+0.00001)
Y = IPRED + W
W = EPS(5)
IRES = DV - IPRED
ENDIF

IF(W.EQ.0)W=1
IWRES = IRES/W

$THETA
(0, 0.58)        ; 1 KE
(0, 0.325)       ; 2 V2
(0, 0.355)       ; 3 KA
(0, 0.178)       ; 4 KA_GI
(1, 7.45)        ; 5 KA_HPF
(0, 0.093)       ; 6 KG
(0, 1.6)         ; 7 *1e1 INOC
(0, 0.991)       ; 8 /1e2 SLP

$OMEGA 1.64      ;IIV INOC
```

```
$OMEGA 0.227    ;IIV SLP

$SIGMA 0.0611   ; 1 prop homogenate INH
$SIGMA 0.59     ; 2 add homogenate INH
$SIGMA 0.485    ; 3 prop blood INH
$SIGMA 0 FIX    ; 4 add blood INH
$SIGMA 0.125    ; 5 prop bacterial burden

$ESTIMATION METHOD=1 INTER MAXEVAL=8000 NOABORT PRINT=10 NSIG=3 SIGL=9
POSTHOC
$COVARIANCE PRINT=E

$TABLE ID TIME KIN KA TVKA KE V2 KA_GI KA_HPF KG INOC SLP C V ETA(1) ETA(2)
DV EVID MDV CMT BQL AQL DOSE AGE AGE_H BLOOD XEXP FLAG IPRED IRES IWRES
CWRES NOPRINT ONEHEADER FILE=tab1
```

## 10.12 NONMEM model code translation to humans of isoniazid response

```
$PROBLEM TRANSLATION

$INPUT ID TIME AMT DV EVID MDV CMT WT METAB DOSE
$DATA TRANSLATE_dataset.csv IGNORE=@

; time in hours
; amt in mg
; dv in mg/L (--> transform linear slope from zebrafish in uM)
; subjects are all male and HIV negative (no covariates)
; METAB is 1 for fast and 0 for slow metabolizers

$SUBROUTINE ADVAN13 TOL=9

$MODEL

COMP(ABS DEFDOSE)
COMP(CENTRAL DEFOBS)
COMP(PERIPH)
COMP(BAC)

$PK

;PK (simulated from Wilkins et al, Br. J. Clin. Pharmacol. 72, 51–62
(2011))

;typical values
TVKA = THETA(1)      ;typical value absorption rate constant
TVALAG2 = THETA(2)   ;typical value absorption lag time to compartment 2
```

```
TVV2 = THETA(3)      ;typical value distribution volume central compartment
TVV3 = THETA(4)      ;typical value distribution volume peripheral compart-
ment
TVQ = THETA(5)       ;typical value intercompartmental clearance

TVCLS = THETA(6)     ;typical value clearance slow metabolizers
TVCLF = THETA(7)     ;typical value clearance fast metabolizers

;PK parameters

KA = TVKA
ALAG2 = TVALAG2 * EXP(ETA(1))
V2 = TVV2 * (WT/70)**1.00 * EXP(ETA(2))
V3 = TVV3 * (WT/70)**1.00
Q = TVQ * EXP(ETA(3))
CLS = TVCLS * (WT/70)**0.75 * EXP(ETA(4))
CLF = TVCLF * (WT/70)**0.75 * EXP(ETA(4))

;microconstants

KEF = CLF / V2
KES = CLS / V2
KE = KES * (1 - METAB) + KEF * (METAB)  ;distinguish between fast and slow
metabolizer
K23 = Q / V2
K32 = Q / V3

S2 = V2

;PD (from PKPD model of isoniazid in zebrafish)

;estimated exponential growth (kg = 0.093007) is used to backcalculate -48h
from inoculum (inoc = 16.276) which is moment of infection in zebrafish with
200 CFU M marinum
;and subsequently to CFU/mL

FL_start = 16.276 * exp(-48 * 0.093007)
CFU_start = 200
f_FL_CFU = CFU_start/FL_start   ;factor to convert fluorescence to CFU
CFU_INOC = 16.276 * f_FL_CFU
f_INOC_CFU = 4888538/CFU_INOC   ;mean inoculum from digitized papers

TVKG = THETA(8)      ;exponential growth rate
TVINOC = THETA(9)    ;inoculum estimated
TVSLP = THETA(10)    ;slope (linear drug effect)

KG = TVKG
INOC = TVINOC * EXP(ETA(5))
SLP0 = TVSLP * EXP(ETA(6))

A_0(4) = INOC * f_FL_CFU * f_INOC_CFU  ;inoculum in CFU/mL

$DES

DADT(1) = -KA * A(1)
DADT(2) = KA * A(1) - KE * A(2) - K23 * A(2) + K32 * A(3)
DADT(3) = K23 * A(2) - K32 * A(3)

C = A(2)/V2

;translational factors (Wicha et al, Clin. Pharmacol. Ther. 104:6, 1208-
1218 (2018))
```

```
;1. MIC
MIC_fac = 0.2/15         ;correct for MIC of INH for MTB (0.2 mg/L, break-
point MIC from Schön et al, J. Antimicrob. Chemother. 64, 786–793 (2009))
in comparison to MM (15 mg/L) by increasing sensitivity

;2. Stage of infection
INFEC_fac = 22.2/8.55  ;correct for difference in effect on logarithmic (ze-
brafish infection, mostly F) and stationary (clinical infection, mostly S
and N) by taking ratio of maximal kill rate
of isoniazid on F and S state (no isoniazid quantified on N state, Clewe et
al, J. Antimicrob. Chemother. 73, 437–447 (2018))

SLP = SLP0 / MIC_fac / INFEC_fac
EFF = SLP * C

DADT(4) = KG * A(4) * (1 - EFF)

$ERROR

IF(CMT.NE.4) THEN
IPRED = LOG(F + 0.0001)
Y = IPRED + EPS(1)
ENDIF

IF(CMT.EQ.4) THEN
IPRED = LOG10(A(4) + 0.0001)
Y = IPRED + EPS(2)
ENDIF

$THETA
1.85             ;1 KA h-1
0.180            ;2 ALAG2 h
57.7             ;3 V2 L
1730             ;4 V3 L
3.34             ;5 Q L/h
9.70             ;6 CLS L/h slow metabolizer
21.6             ;7 CLF L/h fast metabolizer
0.093007         ;8 KG
16.276           ;9 INOC
0.07227485       ;10 SLP 0.0099117/0.137139 (convert slope from uM to mg/L
by dividing by mol. weight)

$OMEGA
0.781456         ;IIV ALAG2 reported %CV 88.4
0.027225         ;IIV V2 reported %CV 16.5
0.866761         ;IIV Q reported %CV 93.1
0.033856         ;IIV CL reported %CV 18.4
1.64             ;IIV INOC
0.227            ;IIV SLP

$SIGMA
0.042025         ;additive on natural log scale, sd = 0.205 mg/L
0.124            ;additive on natural log scale

$SIMULATION (12345) ONLYSIM SUBPROBLEM=1

$TABLE ID TIME AMT DV EVID MDV CMT WT METAB DOSE
TVKA TVALAG2 TVV2 TVV3 TVQ TVCLS TVCLF TVKG TVINOC TVSLP
KA ALAG2 V2 V3 Q CLS CLF KG INOC SLP SLP0 f_FL_CFU ETA1 ETA2 ETA3 ETA4 ETA5
ETA6 IPRED NOPRINT ONEHEADER FILE=tabsim1
```